JOC*Article*

Spectral and Acid−Base Features of 3,7-Dihydroxy-2,8-diphenyl-4*H*,6*H*-pyrano[3,2-*g*]chromene-4,6-dione (Diflavonol)—A Potential Probe for Monitoring the Properties of Liquid Phases

A. D. Roshal,[†] V. I. Moroz,[†] V. G. Pivovarenko,[‡] A. Wróblewska,[§] and J. Błażejowski*[,§]

Institute of Chemistry, Kharkiv V.N. Karazin National University, Svoboda 4, 61077 Kharkiv, Ukraine, Faculty of Chemistry, Kyiv Taras Shevchenko National University, Volodymyrska 64, 01033 Kyiv, Ukraine, and Faculty of Chemistry, University of Gdańsk, J. Sobieskiego 18, 80-952 Gdańsk, Poland

bla@chem.univ.gda.pl

Received February 14, 2003

Diflavonol is a molecule that can exist in neutral or anionic form and in several tautomeric forms in ground and excited states. Absorption and emission spectroscopy combined with theoretical calculations have shown that only one tautomer of neutral diflavonol exists in the ground state, but two exist in the excited state. In the latter case, one is the tautomer originating from the ground state tautomer, which exists in strongly protic solvents, the other is the phototautomer occurring in weakly protic or aprotic solvents as a result of the intramolecular transfer of one proton. The OH groups present in diflavonol and involved in weak intramolecular hydrogen bonds exhibit a proton-donating ability reflected by the experimental values of acidity constants or theoretical enthalpies and free energies of proton detachment. The electronically excited molecule is a relatively strong acid when it loses one proton. With increasing basicity of the medium, monoanionic and dianionic forms occur which exhibit spectral characteristics and an emission ability different from those of neutral diflavonol. These interesting features of diflavonol open up possibilities for the analytical use of the compound and its application as a spectral probe sensitive to the properties of liquid phases.

1. Introduction

The term Excited-State Intramolecular Proton Transfer (ESIPT) was first introduced by Sengupta and Kasha to describe phototautomerization in 3-hydroxy-2-phenyl-4*H*-chromen-4-one (flavonol, **1**) (Chart 1).[1] The most interesting feature of flavonol and its derivatives is the sensitivity of their fluorescence to proton-donating or proton-accepting properties, as well as the polarity of the environment.[1−3] The two bands appearing in the spectra of flavonols have been ascribed to the emission of the normal (**N**), short-wavelength, and the tautomeric (**T**), long-wavelength, forms. The ESIPT effect in flavonols makes the compounds convenient fluorescent probes,[4−8]

CHART 1. Canonic Structures of 3-Hydroxy-2-phenyl-4*H*-chromen-4-one (flavonol) (1) in N and T Forms, and 3,7-Dihydroxy-2,8-diphenyl-4*H*,6*H*-pyrano[3,2-*g*]chromene-4,6-dione (diflavonol) (2) with the Numbering of Atoms Indicated

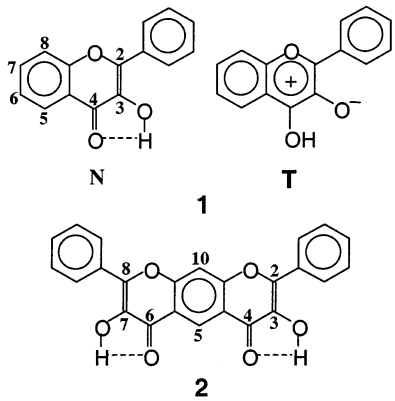

and provides an opportunity to investigate amplified spontaneous emission.[9,10] This effect also influences the

* Corresponding author. Phone: +48 58 345 03 31. Phone/fax: +48 58 345 04 64.
[†] Kharkiv V.N. Karazin National University.
[‡] Kyiv Taras Shevchenko National University.
[§] University of Gdańsk.

(1) Sengupta, P. K.; Kasha, M. *Chem. Phys. Lett.* **1979**, *68*, 382.
(2) Le Gourrierec, D.; Ormson, S. M.; Brown, R. G. *Prog. React. Kinet.* **1994**, *19*, 211.
(3) Formosinho, J. S.; Arnaut, G. L. *J. Photochem. Photobiol. A: Chem.* **1993**, *75*, 21.
(4) Sytnik, A.; Gormin, D.; Kasha, M. *Proc. Natl. Acad. Sci. U.S.A.* **1994**, *91*, 11968.
(5) Pivovarenko, V. G.; Tuganova, A. V.; Klimenko, A. S.; Demchenko, A. D. *Cell. Mol. Biol. Lett.* **1997**, *2*, 355.
(6) Bondar, O. P.; Pivovarenko, V. G.; Rowe, E. S. *Biochim. Biophys. Acta* **1998**, *1369*, 119.
(7) Duportail, G.; Klymchenko, A. S.; Mely, Y.; Demchenko, A. P. *FEBS Lett.* **2001**, *508*, 196.
(8) Demchenko, A. P.; Klymchenko, A. S.; Pivovarenko, V. G.; Ercelen, S. In *Fluorescence Spectroscopy, Imaging and Probes: New Tools in Chemical, Physical and Life Sciences*; Kraayenhof, R., Visser, A. J. W. G., Eds.; Vol. 2, Springer Series on Fluorescence; Sprigner-Verlag: Berlin, Heidelberg, Germany, 2002; p 101.

10.1021/jo034200f CCC: $25.00
Published on Web 06/21/2003

complexing ability of electronically excited flavonol derivatives containing crown macrocycles.[11,12] The proton-donating ability of flavonols has been utilized in investigations of the constitution of mixed liquid phases,[13] the nature of micelles,[5,14] as well as the properties of liposomes[6,15] or proteins.[16]

Searching for flavonol derivatives with potentially more interesting properties, we turned our attention to 3,7-dihydroxy-2,8-diphenyl-4*H*,6*H*-pyrano[3,2-*g*]chromene-4,6-dione (diflavonol,[17] **2**) (Chart 1), first described, to the best of our knowledge, by Algar and Hurley.[18] The spectral and acid−base features of **2** and its derivatives should be more sensitive to changes in the properties of liquid phases, as they contain two potential ESIPT sites. Thus, one can expect in this compound absorption and emission abilities that are enhanced relative to those of flavonol, and a more distinct separation of the fluorescence bands, as we recently found when analyzing the properties of 2,8-bis[4-(diethylamino)phenyl]-3,7-dihydroxy-4*H*,6*H*-pyrano[3,2-*g*]chromene-4,6-dione (the diethylamino derivative of **2**).[19] This creates an opportunity for examining how **2** behaves in comparison with **1** and for discovering the nature of excited states that emit radiation. A further aim of these investigations was to indicate, by investigating the spectral and acid−base features of **2**, the possible applications of the compound in domains where the simpler flavonol molecule may be ineffective.

2. Experimental Section

2.1. Synthesis. 2 was synthesized as described in refs 18 and 20. The compound was purified by repeated recrystallization from chloroform (mp of the yellow crystals was 323−324 °C; lit.[18] mp 323 °C). Its purity was controlled by TLC and ^{1}H NMR spectroscopy: δ 9.77 (2H, s), 8.76 (1H, s), 8.22 (4H, d, 8.0), 8.02 (1H, s), 7.53−7.59 (6H, m) in DMSO-d_6.

2.2. Spectroscopic Investigations. Spectral grade solvents (distilled and dried before use if necessary) were used throughout. The optical path length in all experiments was 1 cm. Concentrations of **2** were in the range 5×10^{-6} to 10^{-5} M in absorption and fluorescence investigations, and ca. 5×10^{-5} M in acid−base titrations.

Solid solutions of **2** in polymeric matrices were obtained by mixing dilute solutions of the compound in dichloromethane with solutions of a polymer in organic solvents (polystyrene in toluene, poly(butyl methacrylate) in butyl acetate); these mixtures were allowed to dry during the following 3−4 days. Poly(vinyl alcohol) was in contact with the methanol solution of **2** during 24 h and the swollen polymer with the absorbed compound was washed with methanol and dried.

The spectral characteristics of particular forms of **2** were extracted from experimental absorption and fluorescence spectra with the Spectral Data Lab program.[21] The scalar difference and angle between the dipole moment vectors of the chromophore and fluorophore fragments was derived by using the Bakhshiyev equation.[22] The above-mentioned angle was also evaluated on the basis of fluorescence anisotropy values employing the formula indicated in ref 23.

2 in methanol and water−ethanol (v/v 1/1) media was titrated against potassium hydroxide, and in acetone against tetrabutylammonium hydroxide ([NBu$_4$]OH).[24] In the latter case, the base was extracted from a commercially available 10% aqueous solution into dichloromethane, after which the extract was dried and diluted 100 times with dry acetone. The concentration of tetrabutylammonium hydroxide in acetone was determined by potentiometric titration with aqueous HCl solution.

The concentration dissociation constants (K_a) of **2** in acetone and methanol were obtained according to the equation $pK_a = pK_s - pK_{OH}$, where p denotes the negative base-10 logarithm, K_{OH} is the concentration basicity constant, and K_s is the ionic product of the solvent. The values of pK_s for the solvents used were taken from refs 25 and 26. Concentration dissociation constants (K_a) in water−ethanol media were obtained by acid−base titrations. Equilibrium constants were derived by employing the method described in ref 24 and the Spectral Data Lab program.[21]

Dissociation constants of the diflavonol hydroxy groups in the excited state were estimated by Förster's method on the basis of the positions of the long-wavelength maxima in the absorption spectra of the neutral and anionic forms.[27,28]

2.3. Calculations. Unconstrained geometry optimizations of isolated molecules (given in Chart 2) in the ground (S_0) and excited singlet (S_1) electronic states were carried out at the semiempirical AM1 (S_0 state) and AM1/CI (S_1 state) levels of theory,[29] with standard procedures being employed together with the BFGS method[30−33] implemented in the MOPAC 93 program package.[34] Solvent (CH_2Cl_2, CH_3CN) effects were included in the ground-state geometry optimizations through the COSMO model (the solvent radii used were 1.81 and 1.27 for CH_2Cl_2 and CH_3CN, respectively).[34,35] The final values of the energy gradient were always lower than 0.1 kcal/mol, and the eigenvalues of the Hessian matrix were all positive. The thermochemical ($\Delta_{f,298}H°$, $_{298}S°$) or physicochemical (HOMO and LUMO energies, dipole moments) characteristics of the compounds were either extracted directly from data files following geometry optimizations[34,36] or obtained from those

(9) Shou, P.; McMorrow, D.; Aarstma, T. J.; Kasha, M. *J. Phys. Chem.* **1984**, *88*, 4596.
(10) Parthenopoulos, D.; Kasha, M. *Chem. Phys. Lett.* **1988**, *146*, 77.
(11) Roshal, A. D.; Grigorovich, A. V.; Doroshenko, A. O.; Pivovarenko, V. G.; Demchenko, A. P. *J. Phys. Chem.* **1998**, *102*, 5907.
(12) Roshal, A. D.; Grigorovich, A. V.; Doroshenko, A. O.; Pivovarenko, V. G.; Demchenko, A. P. *J. Photochem. Photobiol. A: Chem.* **1999**, *127*, 89.
(13) Liu, W.; Wang, Yi.; Jin, W.; Shen, G.; Yu, R. *Anal. Chim. Acta* **1999**, *383*, 299.
(14) Dennison, S. M.; Gubaray, J.; Sengupta, P. K. *Spectrochim. Acta, Part A* **1999**, *55*, 903.
(15) Dennison, S. M.; Gubaray, J.; Sengupta, P. K. *Spectrochim. Acta, Part A* **1999**, *55*, 1127.
(16) Demchenko, A. P. *Biochim. Biophys. Acta* **1994**, *1209*, 149.
(17) Falkovskaia, E.; Pivovarenko, V. G.; del Valle, J. C. *Chem. Phys. Lett.* **2002**, *352*, 415.
(18) Algar, J.; Hurley, D. E. *Proc. R. Ir. Acad., Sect. B* **1936**, *43*, 83.
(19) Pivovarenko, V. G.; Jozwiak, L.; Blazejowski, J. *Eur. J. Org. Chem.* **2002**, 3979.
(20) Smith, M. A.; Neumann, R. M.; Webb, R. A. *J. Heterocycl. Chem.* **1968**, *5*, 425.
(21) Doroshenko, A. O. *Spectral Data Lab Software*; Kharkiv, Ukraine, 1999.
(22) Bakhshiyev, N. G. *Opt. Spectrosc.* **1961**, *10*, 717.
(23) Lakowicz, J. R. *Principles of Fluorescence Spectroscopy*, 2nd ed.; Kluwer Academics Plenum Publishers: New York, 1999.
(24) Bernstein, I. Y.; Kaminsky, Y. L. *Spectrophotometric analysis in organic chemistry*; Khimiya: Leningrad, Russia, 1986; p 140.
(25) Alexandrov, V. V. *Acidity of non aqueous solutions*; Vyshcha Shkola: Kharkov, Ukraine, 1981; p 152.
(26) Kreshkov, A. P.; Aldarova, N. S.; Tanganov, B. V. *Zh. Fiz. Khim.* **1970**, *44*, 2089.
(27) Forster, T. *Z. Elektrochem.* **1950**, *54*, 42.
(28) Martynov, I. Y.; Demiashkevich, A. B.; Uzhinov, B. M.; Kuzmin, M. G. *Usp. Khim.* **1977**, *46*, 3.
(29) Dewar, M. J. S.; Zoebisch, E. G.; Healy, E. F.; Stewart, J. P. P. *J. Am. Chem. Soc.* **1985**, *107*, 3902.
(30) Broyden, C. G. *J. Inst. Math. Appl.* **1970**, *6*, 222.
(31) Fletcher, R. *Comput. J.* **1970**, *13*, 317.
(32) Goldfarb, D. *Math. Comput.* **1970**, *24*, 23.
(33) Shanno, D. F. *Math. Comput.* **1970**, *24*, 647.
(34) Stewart, J. P. P. MOPAC 93; Copyright Fujitsu: Tokyo, Japan, 1993.
(35) Klamt, A.; Schuurmann, G. Z. *J. Chem. Soc., Perkin Trans. 2* **1993**, 799.
(36) Stewart, J. P. P. *J. Comput.-Aided Mol. Des.* **1990**, *4*, 1.

CHART 2. Canonic Structures of Neutral (NN, NT, and TT), Monoanionic (NA and TA), and Dianionic (AA) Forms of 2

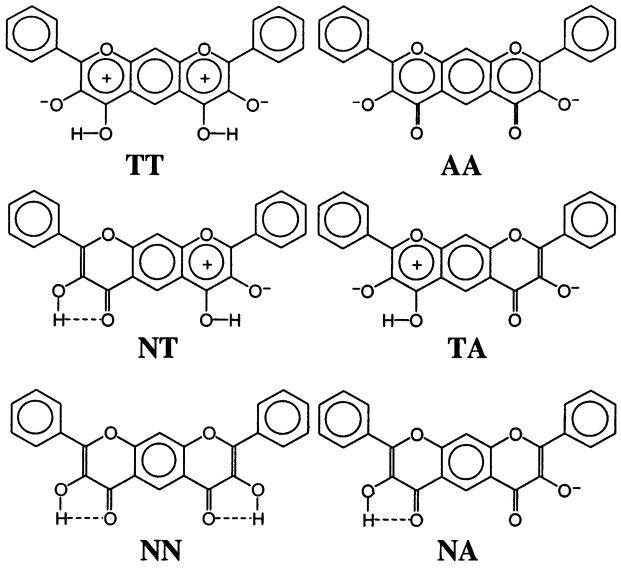

available in MOPAC 93 routines (Mulliken charges[37]). The wavelengths and oscillator strength of electronic transitions were calculated by using ground state (for $S_0 \rightarrow S_1$ transition) or excited state (for $S_1 \rightarrow S_0$ transition) geometries and MOPAC 93[34] or HyperChem[38] program packages. Generally, 201 ground and single excited-state configurations due to excitation within the HOMO-10 and LUMO+10 molecular orbitals were used.[39] Solvent effects were included in the prediction of electronic transitions within the COSMO model.[35]

Geometry optimizations were also carried out at the DFT level of theory,[40] using the B3LYP functional[41,42] and 6-31G** basis set[43,44] implemented in the GAUSSIAN 98 program package.[45] The influence of the solvent was included at the level of the Polarized Continuum Model (PCM) (UAHF radii were used to obtain molecular cavity).[46,47] After completion of each optimization, the Hessian matrix was calculated and the eigenvalues were all positive. From these eigenvalues harmonic vibrational frequencies and then zero-point energy, entropy, enthalpy, and Gibbs' free energy contributions at 298.15 K and standard pressure were calculated, with the aid of a built-in computational program statistical thermodynamics routine.[48] Enthalpies and Gibbs' free energies of formation were calculated by following the basic rules of thermodynamics,[49,50] i.e., the enthalpies (Gibbs' free energies) of gaseous H_2, O_2, and solid C (values of the last quantity were obtained by subtracting the enthalpy or Gibbs' free energy of atomization equal to 171.29 and 160.44 (298.15 K, standard pressure) kcal/mol,[51] respectively, from the data of the gaseous entity), multiplied by the relevant stoichiometric coefficients, were subtracted from the enthalpies (Gibbs' free energies) of gaseous **2**. Dipole moments were extracted directly from data files following the geometry optimizations. DFT calculations were carried out on the computers of the Tri-City Academic Network Computer Centre (TASK) in Gdańsk (Poland).

TABLE 1. Spectral Data for 2 in Liquid Phases and Solid Matrices[a]

medium	λ_{abs}	λ_{fl}(I)	$\Delta\nu_{St}$(I)	λ_{fl}(II)	$\Delta\nu_{St}$(II)	φ
toluene	381	452[b]	4130[b]	602	9630	0.44
trichloroethylene	382	461[b]	4480[b]	595	9360	0.59
1,2-dibromobenzene	382	479[b]	5300[b]	607	9690	0.39
dichloromethane	382	496[b]	6060[b]	598	9480	0.80
acetone	382	510[b]	6580[b]	614	9900	0.25
acetonitrile	379	511[b]	6780[b]	610	9980	0.25
isopentanol	382	508	6510	614	9900	0.005
methanol	380	520	7100			<0.001
polystyrene				598		
poly(butyl methacrylate)				606		
poly(vinyl alcohol)		493		598		

[a] λ_{abs} = position of the maximum of the long-wavelength absorption band, in nm; λ_{fl}(I) and λ_{fl}(II) = positions of the maxima, in nm, of emission bands I and II; $\Delta\nu_{St}$(I) and $\Delta\nu_{St}$(II) = Stokes shifts for emission bands I and II, in cm^{-1}; φ = fluorescence quantum yield (in aprotic solvents, for band II only; in methanol, for band I only; in isopentanol, for both bands). [b] The band appears in aprotic solvents in the presence of traces of proton-donating methanol.

3. Results and Discussion

3.1. Electronic Absorption and Emission Spectroscopy. The electronic absorption spectra of **2** always exhibit two bands between 340 and 420 nm, whose positions depend only slightly and nonsystematically on the properties of the organic solvents; the positions of the long-wavelength maxima differ by less than 3 nm (Table 1).

The fluorescence spectra of **2** in aprotic solvents always contain one narrow band with a maximum between 595 and 614 nm: at a lower wavelength in less polar media and at a higher wavelength in more polar media (Figure 1A). An increase in solvent polarity leads to a decrease in emission intensity. The addition of small amounts (~0.5% v/v) of protic solvents (isopentanol, methanol) to the aprotic ones results in the appearance of a new emission band between 420 and 540 nm (Table 1). The short-wavelength emission, with a maximum at 520 nm, is the only one to appear in the fluorescence spectrum of **2** in methanol, whereas the spectrum in isopentanol exhibits two short- and long-wavelength emission bands. The fluorescence quantum yield decreases sharply with

(37) Mulliken, R. S. *J. Chem. Phys.* **1955**, *23*, 1833, 1841.
(38) HyperChem 5.0; Hypercube Inc: Waterloo, ON, Canada, 1995.
(39) Armstrong, D. R.; Perkins, P. G.; Stewart, J. J. P. *J. Chem. Soc., Faraday Trans. 2* **1972**, *68*, 1939.
(40) Labanowski, J. K. In *Density Functional Methods in Chemistry*; Andzelm J. W., Ed.; Springer-Verlag: New York, 1991.
(41) Becke, A. D. *J. Chem. Phys.* **1993**, *98*, 1371, 5648.
(42) Lee, C.; Yang, W.; Parr, R. G. *Phys. Rev. B* **1988**, *37*, 785.
(43) Francl, M. M.; Pietro, W. J.; Hehre, W. J.; Binkley, J. S.; Gordon, M. S.; DeFrees, D. J.; Pople, J. A. *J. Chem. Phys.* **1972**, *77*, 3654.
(44) Hariharan, P. C.; Pople, J. A. *Theor. Chim. Acta* **1973**, *28*, 213.
(45) Frish, M. J.; Trucks, G. W.; Schlegel, H. B.; Scuseria, G. E.; Robb, M. A.; Cheeseman, J. R.; Zakrzewski, V. G.; Montgomery, J. A., Jr.; Stratmann, R. E.; Burant, J. C.; Dapprich, S.; Millam, J. M.; Daniels, A. D.; Kudin, K. N.; Strain, M. C.; Farkas, O.; Tomasi, J.; Barone, V.; Cossi, M.; Cammi, R.; Mennucci, B.; Pomelli, C.; Adamo, C.; Clifford, S.; Ochterski, J.; Petersson, G. A.; Ayala, P. Y.; Cui, Q.; Morokuma, K.; Malick, D. K.; Rabuck, A. D.; Raghavachari, K.; Foresman, J. B.; Cioslowski, J.; Ortiz, J. V.; Baboul, A. G.; Stefanov, B. B.; Liu, G.; Liashenko, A.; Piskorz, P.; Komaromi, I.; Gomperts, R.; Martin, R. L.; Fox, D. J.; Keith, T.; Al-Laham, M. A.; Peng, C. Y.; Nanayakkara, A.; Challacombe, M.; Gill, P. M. W.; Johnson, B.; Chen, W.; Wong, M. W.; Andres, J. L.; Gonzalez, C.; Head-Gordon, M.; Replogle, E. S.; Pople, J. A. *GAUSSIAN* 98, Revision A.9; Gaussian, Inc.: Pittsburgh, PA, 1998.
(46) Tomasi, J.; Persico, M. *Chem. Rev.* **1994**, *94*, 2027.
(47) Barone, V.; Cossi, M.; Mennucci, B.; Tomasi, J. *J. Chem. Phys.* **1997**, *107*, 3210.
(48) Dewar, M. J. S.; Ford, G. P. *J. Am. Chem. Soc.* **1977**, *99*, 7822.
(49) Atkins, P. W. *Physical Chemistry*, 5th ed.; Oxford University Press: Oxford, U.K., 1994.
(50) Bouzyk, A.; Jozwiak, L.; Wroblewska, A.; Rak, J.; Blazejowski, J. *J. Phys. Chem. A* **2002**, *106*, 3957.
(51) *Handbook of Chemistry and Physics*, 76th ed.; Lide, D. R., Ed.; CRS Press: Boca Raton, FL, 1995−1996.

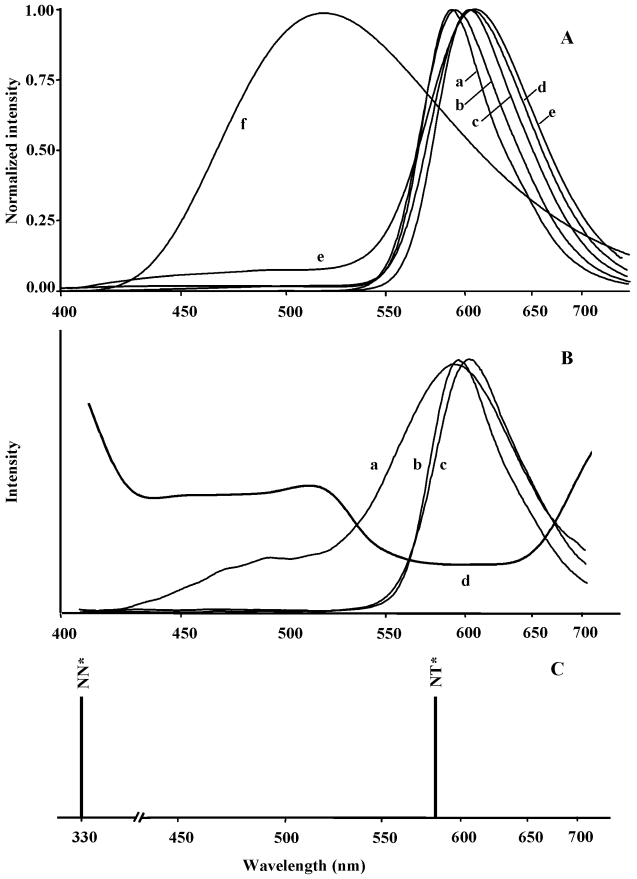

FIGURE 1. Fluorescence spectra of **2**: (A) toluene (a), dichloromethane (b), acetone (c), acetonitrile (d), isopentanol (e), and methanol (f); (B) in poly(vinyl alcohol) (a), polystyrene (b), and poly(butyl methacrylate) (c) together with the anisotropy spectrum in poly(vinyl alcohol) (d); (C) theoretically predicted (AM1/CI level) transitions for the **NN*** and **NT*** forms.

the change from aprotic to protic solvents. In consequence, **2** dissolved in water−ethanol mixtures or water does not exhibit any emission. In polymeric matrices **2** behaves in a similar manner. In aprotic polystyrene and poly(butyl methacrylate) only long-wavelength fluorescence occurs, while in protic poly(vinyl alcohol), an additional short-wavelength emission band appears (Figure 1B).

To discover whether fluorescence spectra bands are single or a superposition of several emissions, we measured the fluorescence anisotropy spectra of **2** in polystyrene, poly(butyl methacrylate), and poly(vinyl alcohol) (Figure 1B). The pattern of these spectra indicates that each fluorescence band is attributable to only one fluorophore. The anisotropy values also enabled us to calculate the angle between the dipole moments of the fluorophore and chromophore: this is approximately 52−53° (54° on the basis of the Bakhshiyev equation[22] and the results of solvatochromic investigations) for the short-wavelength and 59−60° for the long-wavelength emission.

Plotting the Stokes shifts corresponding to the short-wavelength band against media polarity, a straight line is obtained (Figure 2), from which, according to the Bakhshiyev approach,[22] the ratio of dipole moments in

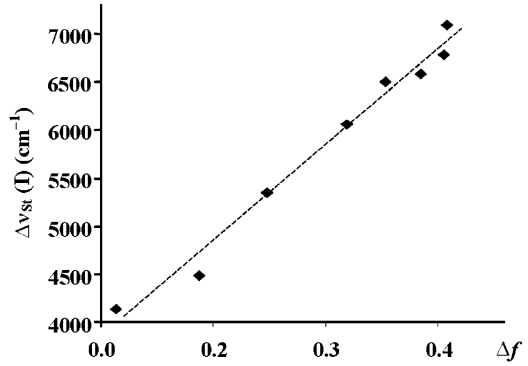

FIGURE 2. Plot of the Stokes shifts of the short-wavelength band in the fluorescence spectra of **2** ($\Delta\nu_{St}$(I)) (Table 1) against the orientational polarizability (Δf) $\Delta f = (\epsilon - 1)/(2\epsilon + 1) - (n^2 - 1)/(2n^2 + 1)$, where ϵ is the dielectric constant and n is the refraction coefficient.

the excited/ground state is calculated to be 1.75. Electronic excitation is, therefore, accompanied by the creation of a nonuniform charge distribution in neutral molecules of **2**.

Spectrophotometric titration of **2** with tetrabutylammonium hydroxide in acetone leads to the appearance of new bands in the long-wavelength region of the absorption spectra with increasing alkali concentration (Figure 3). These bands can be ascribed to monoanionic and dianionic forms of the compound. The pattern of absorption spectra is similar when **2** is titrated against potassium hydroxide in methanol or water−ethanol (v/v 1/1) media, except that the band maxima are shifted toward the short wavelength region (Table 2).

Spectrofluorometric titration of **2** with tetrabutylammonium hydroxide in acetone initially decreases the intensity of emission and shifts the maximum toward the long-wavelength region (619 nm); subsequently, however, the increasing intensity is accompanied by a shift of the maximum toward the short-wavelength region (608 nm) (Figure 4). The fluorescence maximum of neutral **2** falls at 614 nm, and it is thus difficult, on the basis of the positions of the maxima, to differentiate which form emits radiation. To resolve this problem we used the Spectral Data Lab program[21] to deconvolute the absorption and fluorescence spectra recorded after titration; the results are presented in Figure 5. Absorption characteristics indicate that all three forms (neutral, monoanionic, and dianionic) absorb radiation and are consecutively transformed from one into another during titration. On the other hand, only neutral and dianionic forms fluoresce (the former more weakly than the latter: the fluorescence quantum yield of the neutral form is 0.25 (Table 1), that of the dianionic form is 0.41 (Table 2)), while monoanionic forms do not emit radiation.

The very weak fluorescence of **2** in methanol does not increase substantially upon titration with potassium hydroxide, although the emission band is moved 9 nm toward the long-wavelength region (Table 2) relative to that of the neutral form (Table 1). By analogy to what was found in acetone solutions, this emission may be assumed to be associated with the dianionic form.

Neutral **2** does not fluoresce in water−ethanol (v/v 1/1) solution, but does emit very weakly when the medium is

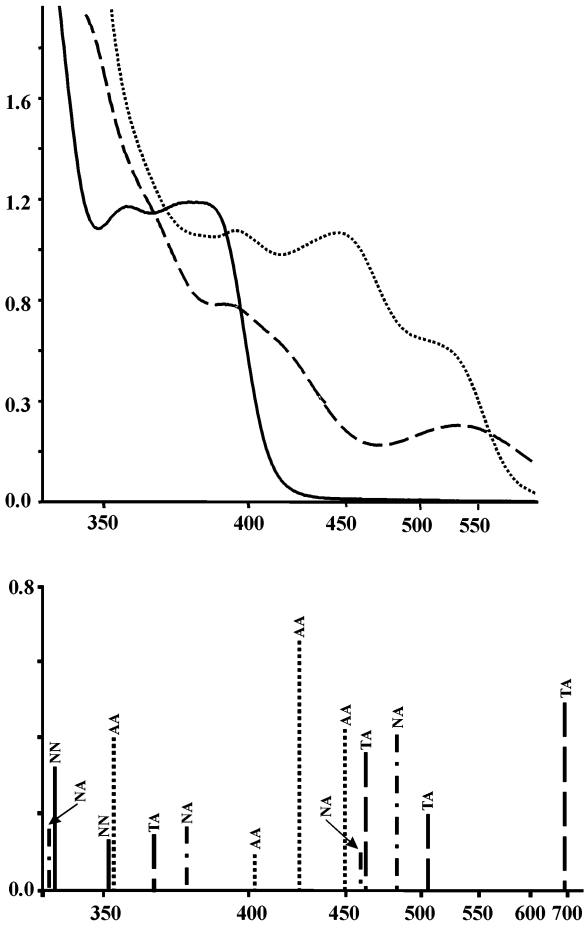

FIGURE 3. Absorption spectra of neutral (—), monoanionic (- - -), and dianionic (···) **2** in acetone (A) together with theoretically predicted (AM1/CI (COSMO) level) absorption transitions in neutral (**NN**), monoanionic (**NA** and **TA**), and dianionic (**AA**) forms (B).

TABLE 2. Spectral Characteristics of Anionic Forms of 2[a]

medium	form	λ_{abs}	log ϵ	λ_{fl}	$\Delta\nu_{St}$	φ
acetone	monoanionic	520	3.54			
	dianionic	514	3.68	608	3000	0.41
methanol	monoanionic	459	3.68			
	dianionic	454	4.17	529	3120	0.03
water−ethanol	monoanionic	473	3.48			
(v/v 1/1)	dianionic	468	4.07	542	2920	>0.005

[a] λ_{abs} = position of the long-wavelength absorption maximum, in nm; ϵ = decadic absorption coefficient, in M^{-1} cm^{-1}; λ_{fl} = position of the fluorescence band maximum, in nm; $\Delta\nu_{St}$ = Stokes shifts ($\lambda_{abs} - \lambda_{fl}$), in cm^{-1}; φ = fluorescence quantum yield.

alkalized (Table 2). This emission can be attributed, as the one in methanol, to the dianionic form.

Absorption and emission bands of the monoanionic and dianionic forms of **2** in methanol are shifted toward the short-wavelength region relative to those in acetone (Table 2), which may be due to methanol's protic properties.

3.2. Proton-Donating Ability. The equilibrium constants corresponding to the detachment of the proton from the neutral **2** (K_a(1)) and monoanionic form of **2** (K_a(2)) in the ground and excited (*) electronic states are given in Table 3. The values of K_a relevant to both states

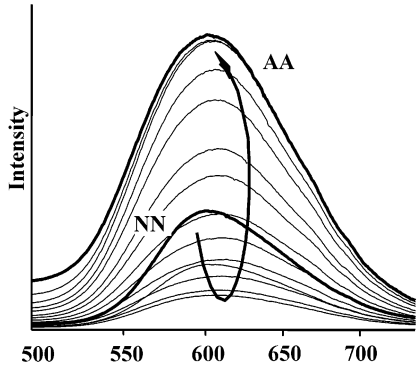

FIGURE 4. Changes in emission upon titration of a solution of **2** in acetone with [NBu_4]OH.

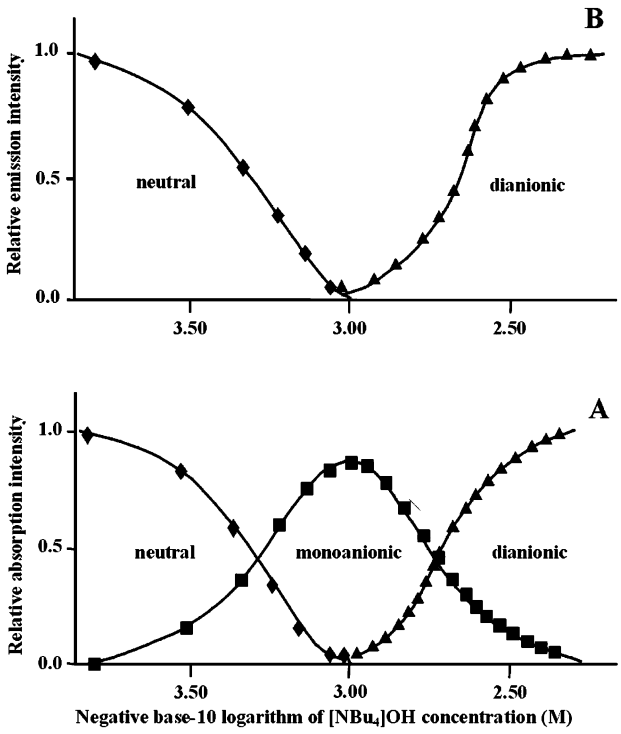

FIGURE 5. Changes in intensities, determined using the Spectral Data Lab program, of the absorption of neutral, monoanionic, and dianionic forms (A) and the fluorescence of neutral and dianionic forms (B) upon titration of solutions of **2** in acetone with [NBu_4]OH.

are highest when the medium is a water−ethanol (v/v 1/1) mixture and lowest when acetone is the solvent. Some of values listed in Table 3 are similar to those found in the case of **1** (in 30% (v/v) ethanol−water pK_a = 9.12 and pK_a* = −1.21[12]). K_a values corresponding to the excited state are generally higher than those for the ground state, which means that excited molecules are stronger acids than neutral ones. This feature may explain the relatively low fluorescence quantum yields in methanol or water−ethanol mixtures as a result of the partial (or total, in the second case) dissociation of **2** to the monoanion. In the case of the ground state, K_a(2) values are roughly 2 orders of magnitude lower than K_a(1), while in the excited state this difference exceeds 10 orders of magnitude. Moreover, pK_a(2) and pK_a(2)* values are high and comparable, which means that the ability to lose the second proton is low in both electronic states.

TABLE 3. Dissociation Constants of 2 in the Ground and Excited (*) States[a]

	S_0			S_1		
medium	$pK_a(1)$	$pK_a(2)$	ΔpK_a	$pK_a(1)^*$	$pK_a(2)^*$	ΔpK_a^*
acetone	21.8 ± 0.1	23.3 ± 0.1	1.5	7.2	24.1	16.9
methanol	13.5 ± 0.1	14.3 ± 0.1	0.8	4.9	15.0	10.2
ethanol−water (v/v 1/1)	9.2 ± 0.1	11.5 ± 0.1	2.3	1.0	12.9	11.9

[a] $pK_a = -\log K_a$; $K_a(1)$ corresponds to the equilibrium neutral **2** ↔ monoanionic **2** + H^+, $K_a(2)$ to monoanionic **2** ↔ dianionic **2** + H^+; $\Delta pK_a = pK_a(2) - pK_a(1)$.

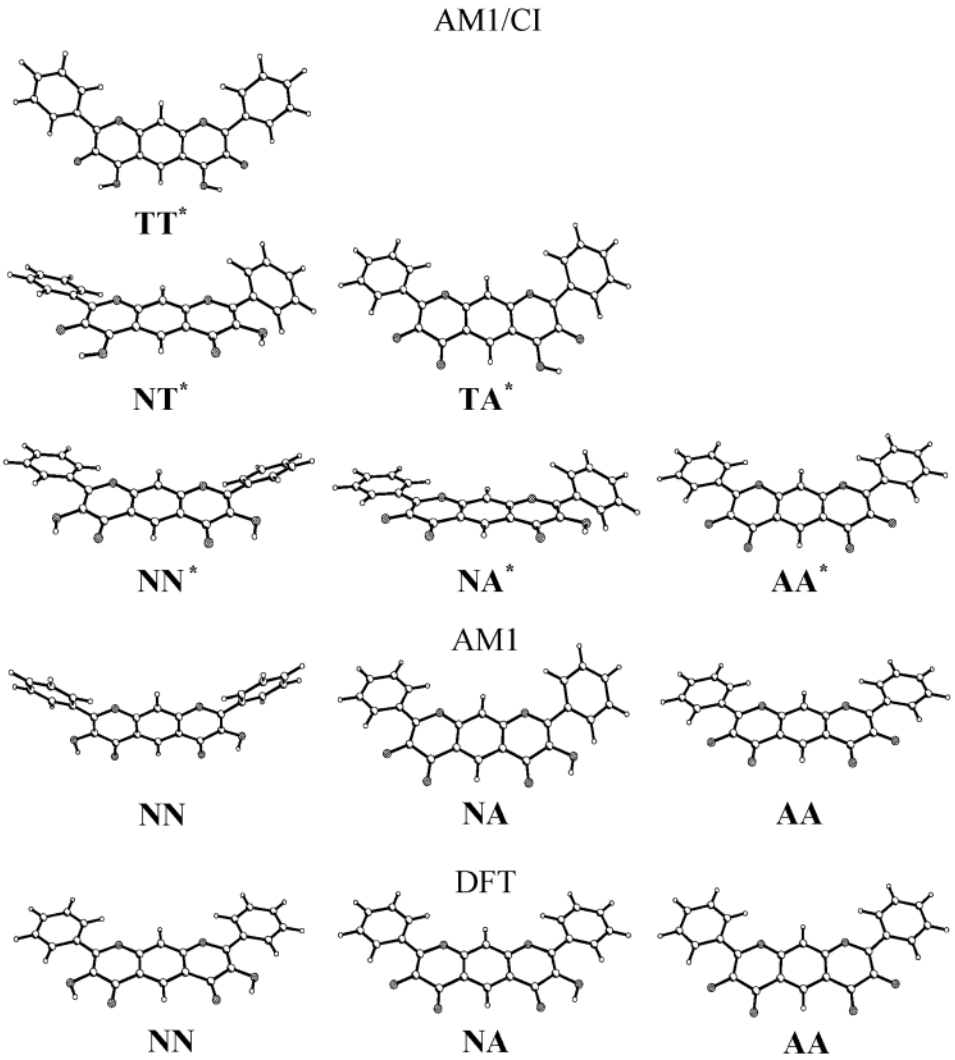

FIGURE 6. DFT, AM1, and AM1/CI optimized structures of neutral, monoanionic, and dianionic forms of **2** in the ground and excited electronic states (for symbols see Chart 2).

The conclusion to be drawn from the above analysis is that **2** exhibits a low ability to lose a proton in the ground state while it is relatively susceptible to losing the first proton in the excited state. This implies that ESIPT is probably associated with the transfer of only one proton in the excited state.[17]

However, the above analysis of experimental data provides no insight into the nature and properties of absorbing and emitting entities. This information can be elicited from the results of the calculations described below.

3.3. Structure and Physicochemical Properties. To interpret the absorption and emission features of **2** it seemed appropriate to consider three canonic structures of the molecule in the ground and excited (*) state (Chart 2) corresponding to the situation without proton transfer (**NN** and **NN***, respectively), with the transfer of one proton (**NT** and **NT***, respectively), and with the transfer of two protons (**TT** and **TT***, respectively),[19] by analogy with what was assumed in the case of **1** (Chart 1). The theoretically predicted structures of these forms are shown in Figure 6 (see also Supporting Information) and the relevant thermochemical and physicochemical data are given in Table 4. The **NT** and **TT** forms exhibit much higher enthalpies and Gibbs' free energies of formation than does the **NN** form, which implies that the latter predominates in the ground electronic state. Both AM1 and DFT methods predict a symmetrical (C_s symmetry)

TABLE 4. Theoretically Predicted Thermochemical and Physicochemical Data for 2[a]

entity (Chart 2)	method	medium	$\Delta_{f,298}H°$ (energy)	$\Delta_{f,298}G°$	$_{298}S°$	energy HOMO	energy LUMO	μ
			S_0 state					
NN	AM1		−90.4		123.4	−9.00	−1.27	4.09
	AM1(COSMO)	CH_2Cl_2	−105.5			−9.11	−1.42	6.40
	AM1(COSMO)	CH_3CN	−110.2			−9.14	−1.44	7.00
	DFT		−71.3	−16.9	162.6			5.02
			(−1374.362620)					
NT	AM1		−56.7		122.8	−7.72	−2.24	5.25
	AM1(COSMO)	CH_2Cl_2	−80.8			−8.11	−2.24	8.31
	AM1(COSMO)	CH_3CN	−88.0			−8.22	−2.18	9.28
	DFT		−59.3	−4.5	161.6			5.18
			(−1374.342294)					
TT	AM1		−35.9		121.8	−7.66	−2.71	2.85
	AM1(COSMO)	CH_2Cl_2	−59.0			−8.01	−2.57	1.31
	AM1(COSMO)	CH_3CN	−66.0			−8.09	−2.46	0.53
	DFT		−46.6	8.4	160.7			4.60
			(−1374.320971)					
NA	AM1		−130.4		124.8	−3.88	1.24	
	AM1(COSMO)	CH_2Cl_2	−186.1			−7.14	−0.85	
	AM1(COSMO)	CH_3CN	−198.3			−7.74	−1.19	
	DFT		−97.8	−47.8	162.0			
			(−1373.807736)					
TA	AM1		−130.4		109.7	−4.18	0.45	
	AM1(COSMO)	CH_2Cl_2	−186.1			−7.18	−1.70	
	AM1(COSMO)	CH_3CN	−198.3			−7.75	−1.97	
	DFT		−89.2	−38.9	161.1			
			(−1373.792771)					
AA	AM1		−121.6		122.5	−1.65	4.97	
	AM1(COSMO)	CH_2Cl_2	−258.9			−6.72	0.03	
	AM1(COSMO)	CH_3CN	−285.2			−7.60	−0.81	
	DFT		−71.9	−26.3	161.1			
			(−1373.169458)					
			S_1 state					
NN*	AM1/CI		0.7	126.4	−6.35	−3.76	7.70	
	AM1/CI (COSMO)	CH_2Cl_2	−15.7		−3.84	−1.21	9.27	
	AM1/CI (COSMO)	CH_3CN	−20.8		−3.85	−1.26	9.81	
NT*	AM1/CI		−3.7	123.3	−4.27	−1.01	10.06	
	AM1/CI (COSMO)	CH_2Cl_2	−26.7		−4.35	−1.19	8.96	
	AM1/CI (COSMO)	CH_3CN	−21.4		−4.35	−1.22	8.86	
TT*	AM1/CI		14.8	125.0	−4.47	−1.90	3.63	
	AM1/CI (COSMO)	CH_2Cl_2	−7.7		−4.52	−1.97	3.87	
	AM1/CI (COSMO)	CH_3CN	−13.7		−4.49	−1.98	3.74	
NA*	AM1/CI		−89.2	126.4	−5.47	−2.85		
	AM1/CI (COSMO)	CH_2Cl_2	−142.7		−5.06	−2.74		
	AM1/CI (COSMO)	CH_3CN	−150.2		−5.39	−3.32		
TA*	AM1/CI		−86.0	125.1	−4.42	−2.84		
	AM1/CI (COSMO)	CH_2Cl_2	−128.7		−5.18	−3.50		
	AM1/CI (COSMO)	CH_3CN	−136.8		−4.03	−1.08		
AA*	AM1/CI		−55.6	123.0	−3.56	−1.45		
	AM1/CI (COSMO)	CH_2Cl_2	−193.6		−2.59	−0.30		
	AM1/CI (COSMO)	CH_3CN	−217.5		−3.18	−0.66		

[a] Energy, in hartrees (1 hartree = 627.51 kcal/mol), corresponds to the total electronic energy; $\Delta_{f,298}H°$ and $\Delta_{f,298}G°$, both in kcal/mol, denote standard (°) enthalpy (in solution − AM1(COSMO)) and Gibbs' free energy of formation, respectively; $_{298}S°$, in cal/(mol K), is the entropy; HOMO and LUMO, in eV, indicate the energies of the highest occupied and lowest unoccupied molecular orbitals; μ, in D, is the dipole moment.

structure for the **NN** form (Figure 6) and that the atomic charge distribution in it is symmetrical (Figure 7). The symmetrical structure of **2** is also reflected in the symmetrical pattern of experimental ^{1}H NMR signals (which is demonstrated in the Experimental Section). In the first excited singlet state (S_1), enthalpies of formation follow the order **TT*** > **NN*** > **NT***, which differs from that obtained at the DFT (B3LYP)/CIS level, **NN*** > **TT*** > **NT*** (**NN*** is predicted to be 12.3 kcal/mol less stable than **TT*** and 21.7 kcal/mol less stable than **NT***).[17] As the latter information was rather unexpected we decided to use data obtained from the AM1/CI calculations, which correspond better to our experimental results. Absorption of radiation is accompanied with excitation of **NN** to **NN***, and the latter can easily be transformed, according to the results of our calculations, to the lower energy **NT*** form. On the other hand, the **NN*** → **TT*** transformation would require extra energy, so the appearance of the **TT*** form is not likely. This implies that only **NN*** and **NT*** forms are present in the S_1 state. None of the three excited state forms are symmetrical (Figure 6), since the electronic transitions are accompanied by the generation of nonsymmetrical charge distribution in the molecules, as Figure 7 demonstrates.

In alkaline media, **2** can exist in monoanionic and dianionic forms. The two possible monoanionic structures (Chart 2) exhibit a comparable thermodynamic stability in the ground (**NA** and **TA**) and excited (**NA*** and **TA***)

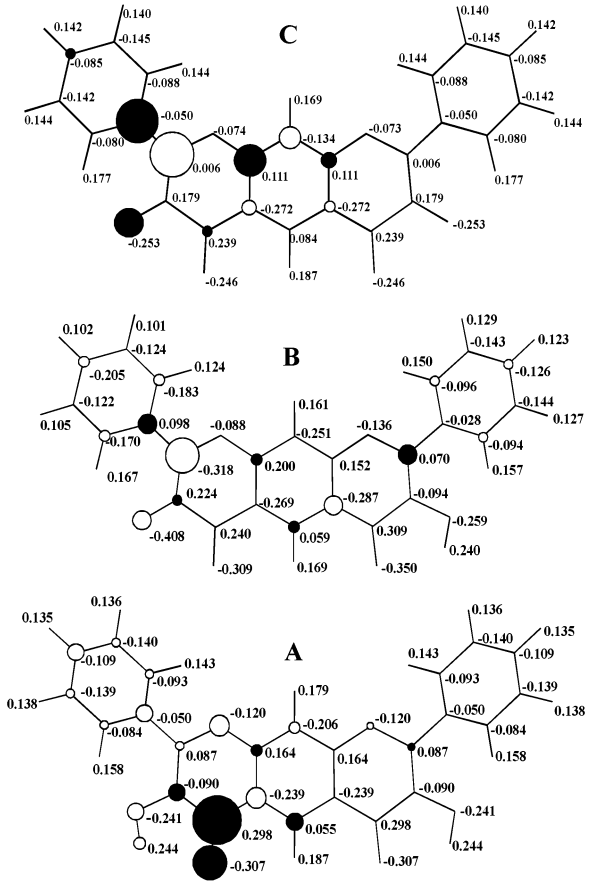

FIGURE 7. Atomic partial charges of **2** (**NN**) (A), monoanionic **2** (**NA**) (B), and dianionic **2** (**AA**) (C) in the ground electronic state (given as numbers at atoms) together with differences of these charges relevant to electronic excitation (open circles indicate a decrease in negative charge upon excitation, the filled circles an increase in this charge; the size of the circles is proportional to the difference in the respective charges obtained at the AM1/CI and AM1 levels) (for canonic structures, see Chart 2).

electronic states, according to the results of semiempirical calculations (Table 4). DFT data indicate, however, that **NA** should be much more stable than **TA** in the ground state. There is only one dianionic form in the ground (**AA**) and excited (**AA***) state (Chart 2). None of the monoanionic forms are symmetrical, whereas the dianionic form in the ground state is symmetrical (C_s symmetry) (Figure 6). Electronic transitions are always accompanied by changes in electronic charge distribution (Figure 7).

The results of calculations at the COSMO level demonstrate that inclusion of the medium provides enthalpies of formation in solution that are lower relative to those for the gaseous phase (Table 4). Furthermore, an increase in the polarity of a solvent stabilizes substantially ionic forms—more dianionic and less monoanionic. It is, however, interesting that the differences in the enthalpies of formation of the relevant excited and ground state forms remain comparable and are only slightly affected by the properties of the medium.

Both OH groups in **2** are involved in hydrogen bonds, whose geometry is demonstrated in the Supporting Information (Table S2). These bonds are highly asymmetrical and the H atom is always much closer to one of the O atoms involved in the interactions. Owing to the relatively low values of the OHO angle these interactions may be expected to be rather weak. The geometry of the hydrogen bonds is similar in the ground and excited states, although it can be noted that OH distances are usually somewhat smaller and OHO angles larger in the electronically excited than the ground state, which would imply that hydrogen bonding interactions are more distinct in the former case.

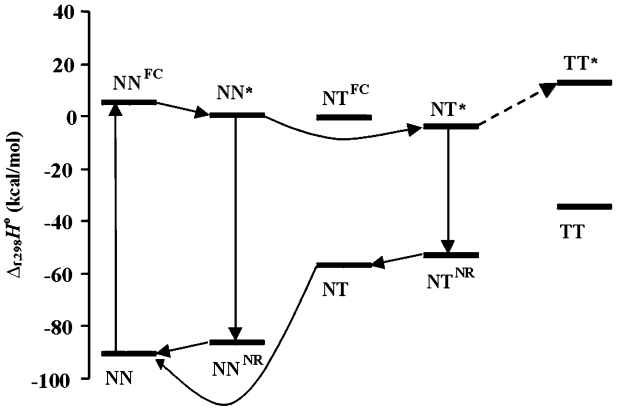

FIGURE 8. Enthalpy changes at the AM1 and AM1/CI level upon excitation, ESIPT, fluorescence, and relaxation in **2** (superscripts **FC** and **NR** denote nonrelaxed excited Franck−Condon and ground states, respectively).

3.4. Origin of Light Absorption and Emission. The similarities of the spectra of neutral **2** in various solvents indicate that only one form participates in the absorption of radiation; according to the results of theoretical calculations, this is **NN**, since the other two tautomeric forms (**NT** and **TT**) are energetically much less stable. Absorption transforms **NN** to the nonrelaxed **NN^{FC}** form which, on losing vibrational energy, achieves the relaxed **NN*** state from which fluorescence occurs (**NN*** → **NN^{NR}**)—if ESIPT is restricted (Figure 8). The latter situation occurs in protic media (Figure 1). In aprotic solvents, however, ESIPT (**NN*** → **NT***) does take place and fluorescence occurs from the relaxed **NT*** state. This long-wavelength fluorescence, characterized by an atypically large Stokes shift (Table 1) (as in the case of **1**[12]), is relatively strong in these solvents but quite weak in a weakly protic solvent such as isopentanol, where both emissions are observed. **NN*** → **NT*** transformation, initiated by electronic excitation of **NN** and accompanied by proton transfer, is thus efficient in aprotic media but is restricted in protic ones. This effect can be explained by strong interactions of the hydrogen bond type between excited **2** and solvent molecules. This renders ESIPT inefficient, but also efficiently deactivates excited molecules, and this in consequence leads to almost complete quenching of emission. These intermolecular hydrogen bonds, which may result in the formation of a cyclic type of conglomerate, compete with the intramolecular ones initially present in **NN***—the precursor of the **NT*** phototautomer.[52]

According to the results of AM1 calculations, two tautomeric forms of monoanionic **2** can coexist in the ground state and absorb radiation (Figure 3). Indeed, titration of neutral **2** with alkalis gives rise to new bands,

(52) McMorrow, D.; Kasha, M. *J. Phys. Chem.* **1984**, *88*, 2225.

TABLE 5. Mulliken Partial Charges (Q) on the Oxygen Atoms of the Hydroxy Groups in Neutral 1 and 2

		1		2		
medium	method	form	Q(3)[a]	form	Q(3)[a]	Q(7)[a]
	AM1	**N**	−0.245	**NN**	−0.241	−0.241
	AM1/CI	**N***	−0.170	**NN***	−0.175	−0.240
	AM1/CI	**T***	−0.323	**NT***	−0.269	−0.242
				TT*	−0.372	−0.372
dichloromethane	AM1	**N**	−0.241	**NN**	−0.266	−0.266
	AM1/CI (COSMO)	**N***	−0.233	**NN***	−0.191	−0.267
	AM1/CI (COSMO)	**T***	−0.396	**NT***	−0.355	−0.267
				TT*	−0.463	−0.463
acetonitrile	AM1	**N**	−0.280	**NN**	−0.278	−0.278
	AM1/CI (COSMO)	**N***	−0.233	**NN***	−0.191	−0.278
	AM1/CI (COSMO)	**T***	−0.414	**NT***	−0.383	−0.279
				TT*	−0.487	−0.487

[a] The number of the carbon atom to which the hydroxy group is attached is given in parentheses (Chart 1).

TABLE 6. Theoretical Enthalpies or Free Energies of Proton Detachment ($\Delta_{d,298}H°$) in the Ground and Excited (*) States[a]

medium	method	$\Delta_{d,298}H°(1)$	$\Delta_{d,298}H°(2)$	ΔpK_a [b]	$[\Delta_{d,298}H°(1)]^*$	$[\Delta_{d,298}H°(2)]^*$	ΔpK_a^* [b]
gaseous	AM1	313.6	362.3	35.7			
	DFT	332.9[c]	385.4[c]	38.5[#]			
	AM1/CI				263.6	387.0	90.4
acetone	AM1 (COSMO)	121.2	123.8	1.93			
	DFT (PCM)	53.3[c]	58.0[c]	3.45[#]			
	AM1/CI (COSMO)				79.3	142.9	46.6
methanol	AM1 (COSMO)	115.7	116.9	0.88			
	DFT (PCM)	31.3[c]	31.9[c]	0.44[#]			
	AM1/CI (COSMO)				75.0	135.5	44.3

[a] For AM1, AM1/CI, AM1 (COSMO) and AM1/CI (COSMO), $\Delta_{d,298}H°(1)$: neutral **2** (**NN**) → monoanionic **2** (**NA**) + H^+; $\Delta_{d,298}H°(2)$: monoanionic **2** (**NA**) → dianionic **2** (**AA**) + H^+. In the case of DFT (PCM), $\Delta_{d,298}H°(1)$: neutral **2** (**NN**) + acetone (or methanol) → monoanionic **2** (**NA**) + [acetone·H]$^+$ (or [methanol·H]$^+$); $\Delta_{d,298}H°(2)$: monoanionic **2** (**NA**) + acetone (or methanol) → dianionic **2** (**AA**) + [acetone·H]$^+$ (or [methanol·H]$^+$); all values in kcal/mol. [b] $\Delta pK_a = [\Delta_{d,298}H°(2) - \Delta_{d,298}H°(1)]/(2.303RT)$ (or $[\Delta_{d,298}G°(2) - \Delta_{d,298}G°(1)]/(2.303RT)$; the value marked [#]), and $\Delta pK_a^* = \{[\Delta_{d,298}H°(2)]^* - [\Delta_{d,298}H°(1)]^*\}/(2.303RT)$. [c] Values represent the Gibbs' free energy (gaseous phase) or solvation free energy (acetone, methanol) change (in kcal/mol) relevant to proton detachment. Total Gibbs' free energies (gaseous phase) or solvation free energies (acetone, methanol), in hartrees (1 hartree = 627.51 kcal/mol), are the following: −1374.090516, −1373.549936, −1372.925702, −0.009999 for **NN**, **NA**, **AA**, H^+ (gaseous phase); −1374.370063, −1373.872404, −1373.367259, −193.167743, −193.580479 for **NN**, **NA**, **AA**, acetone, [acetone·H]$^+$ (acetone); and −1374.387568, −1373.895726, −1373.402912, −115.732405, −116.174392 for **NN**, **NA**, **AA**, methanol, [methanol·H]$^+$ (methanol).

the positions of which qualitatively match the theoretically predicted transitions in **NA** and **TA**. This would mean that proton transfer can occur in the ground state of monoanionic **2**. As the latter entity does not emit radiation (Figure 5), it is difficult to state whether ESIPT takes place in the excited state. Only one form of dianionic **2** is possible according to the results of theoretical calculations. Also, in this case, absorption qualitatively correlates with theoretically predicted transitions.

Experimental emission data (Figure 4) are qualitatively in accordance with the theoretically predicted characteristics of the **NN***, **NT***, **NA***, **TA***, and **AA*** forms of **2** in acetone (respective fluorescence wavelengths: 336, 499, 730, 745, and 550 nm). The lack of emission below 350 nm and above 700 nm indicates that **NN***, **NA***, and **TA*** do not contribute to fluorescence in this solvent. Furthermore, since emission of **NA*** and **TA*** is predicted in the long-wavelength region, these forms may relatively easily lose energy in the nonradiative processes that compete with fluorescence. This is a further explanation why **NA*** and **TA*** do not fluoresce.

Electronic excitation and emission (deactivation) always accompany charge distribution changes (Table 5, Figure 7), which are an attribute of radiative transitions. These changes are reflected in the values of the dipole moment, a macroscopic quantity. Estimates based on experimental spectra make the ratio of excited/ground state dipole moments equal to ca. 1.75, which compares qualitatively with the theoretically predicted ratio of 1.4 (Table 4).

It is also interesting to note that the charges on the oxygen atoms of hydroxy groups change substantially following proton detachment or electronic excitation (Table 5). These charges are only slightly influenced by the environment, which means that the electronic density changes accompanying dissociation or excitation take place mainly within the molecules of **1** or **2**.

3.5. Experimental versus Theoretical Capacity for Proton Detachment (Dissociation). The results of calculations enabled the enthalpies of proton detachment to be predicted in the ground ($\Delta_{d,298}H°$) and excited ($[\Delta_{d,298}H°]^*$) states (Table 6). These characteristics are related qualitatively to the dissociation constants listed in Table 3. Thus, highly positive values of $\Delta_{d,298}H°$ or $[\Delta_{d,298}H°]^*$ mean that a substantial amount of energy must be supplied to the molecule for a proton or protons to be detached. The lower dissociation constants in acetone correlate with the higher enthalpies of proton detachment in this solvent. The greater ability to detach the first proton in the excited state correlates with the lower $[\Delta_{d,298}H°]^*$ values for this process. The higher K_a-(1) in comparison with K_a(2) correlates with the lower

$\Delta_{d,298}H°(1)$ in comparison with $\Delta_{d,298}H°(2)$. The slightly lower $K_a(2)$***** in comparison with $K_a(2)$ corresponds to the higher $[\Delta_{d,298}H°(2)]$***** in comparison with $\Delta_{d,298}H°(2)$. The data in Table 6 indicate, moreover, that it is much easier to detach the first proton from excited than from nonexcited molecules, which additionally confirms that only one proton is transferred in the ESIPT process. It can further be noted that the presence of a medium substantially increases the likelihood of proton detachment ability in **2**—a feature difficult to demonstrate experimentally.

$\Delta_{d,298}G°(1)$ and $\Delta_{d,298}G°(2)$ values predicted at the DFT level (332.9 and 385.4 kcal/mol, respectively) allow ΔpK_a to be calculated (38.5) (gaseous phase) (Table 6). The latter value differs substantially from the experimental ones (Table 3). However, when the solvent is included, ΔpK_a values predicted at both AM1 and DFT level (Table 6) correspond quite well to the experimental ΔpK_a and ΔpK_a***** values (Table 3). This correlation shows that the theory is a useful tool for explaining the features and acid−base behavior of **2**.

4. Concluding Remarks

Only one form of neutral **2** (**NN**) exists in the ground state and absorbs radiation, while in the excited state two forms (**NN*** and **NT***) emit radiation. The less stable form (**NN***) predominates in strongly protic solvents, which interact with it through hydrogen bonds; this restricts ESIPT. The more stable form (**NT***) occurs as a result of ESIPT (**NN*** → **NT*** nonradiative transfer) and fluoresces in weakly protic or aprotic solvents.

The two monoanionic forms of **2** (**NA** and **TA**) most probably coexist in the ground state and both absorb radiation. There is only one dianionic form of **2** and its absorption is stronger than that of the monoanionic forms. The electronically excited dianionic form of **2** (**AA***) fluoresces more strongly than do the neutral forms (**NN*** or **NT***), while the monoanionic forms emit no radiation at all.

Neutral **2** exhibits acidic properties which are associated with the ability to detach protons from the OH groups present in the molecule. This ability is quite low in the ground state, but increases considerably in the excited state, in which the molecule behaves as a relatively strong acid.

The marked influence of the medium on the spectral behavior of **2** makes the compound an interesting probe that can be used to monitor the properties of liquid phases and which can be applied in chemical, biochemical, and environmental analysis.

Acknowledgment. The financial support of this work from the Polish State Committee for Scientific Research (KBN) through the 4 T09A 123 23 (Contract No. 0674/*T*09/2002/23) and BW/8000-5-0281-2 grants, as well as the Polish-Ukrainian Executive Program of Research and Technical Cooperation (Grant No. PRO: III.28/1998; Contract No. 157), is gratefully acknowledged.

Supporting Information Available: Geometries of all stationary points in Cartesian coordinates, energies of stationary points, zero-point energies, and the number of imaginary frequencies; the geometry of intramolecular hydrogen bonds. This material is available free of charge via the Internet at http://pubs.acs.org.

JO034200F